Pakistan Veterinary Journal

ISSN: 0253-8318 (PRINT), 2074-7764 (ONLINE)
DOI: 10.29261/pakvetj/2026.165

RESEARCH ARTICLE

Cyclooxygenase-1 & -2 and Ki67 Expression in Early- and Advanced-Stage Ovine Pulmonary Adenocarcinomas

Mehmet Fatih Bozkurt[1], Emin Karakurt[2], Mudassar Zafar[3*], İsmail Bolat[4], Selim Çomakli[4], Nüvit Coşkun[5], Merve Bolat[6] Serkan Yildirim[4], Enver Beytut[2], Şemistan Kiziltepe[7], Volkan Yilmaz[5], Metin Kiliçlioğlu[4], Emrah Korkulu[5] and Yusuf Tarık Özbay[8]

[1]Department of Pathology, Faculty of Veterinary Medicine, Afyon Kocatepe University, Afyon, Türkiye, 03200; [2]Department of Pathology, Faculty of Veterinary Medicine, Kafkas University, Kars, Türkiye, 36100; [3]University of Veterinary and Animal Sciences, Jhang Campus, Pakistan 35200, Institute of Health Sciences, Afyon Kocatepe University, Afyon, Türkiye, 03200; [4]Department of Pathology, Faculty of Veterinary Medicine, Atatürk University, Erzurum, Türkiye, 25040; [5]Department of Virology, Faculty of Veterinary Medicine, Kafkas University, Kars, Türkiye, 36100;[6]Department of Physiology, Faculty of Veterinary Medicine, Atatürk University, Erzurum, Türkiye, 25040 [7]Medical Services and Techniques Department, Tuzluca Vocational School, Iğdır University, Iğdır, Türkiye, 76100; [8]Institute of Health Sciences, Kafkas University, Kars, Türkiye, 36100
*Corresponding author: mudassarzafar899@gmail.com

ARTICLE HISTORY (26-220)

Received: March 08, 2026
Revised: May 07, 2026
Accepted: May 16, 2026
Published online: July 08, 2026

Key words:
Cyclooxygenases
Immunohistochemistry
Jaagsiekte sheep retrovirus
Ovine pulmonary
Adenocarcinoma
Western blot

ABSTRACT

Ovine pulmonary adenocarcinoma (OPA), is a common disease in places where sheep are reared. Its Diagnosis can be done using histopathology, or through the detection of exJSRV nucleic acid. This study aimed to asses Cyclooxygenase-1 (COX-1) and Cyclooxygenase-2 (COX-2) expression in the early and advanced stages of OPA using immunohistochemistry and Western blotting. Lung tissue samples of eighteen sheep bearing symptoms were investigated for this purpose. Tissues were routinely processed and serial sections were obtained. Haematoxylin & Eosin (H&E) staining, Avidin-Biotin Peroxidase Technique (ABC) with commercial antibodies for JSRV capsid protein (JSRV CA), COX-1, COX-2, and Ki67 was performed on the sections. COX-1, and COX-2 expression levels were determined by Western Blotting. All tissues were tested with RT-PCR and further analyzed for confirmation of exJSRV nucleic acid presence. Nine sheep samples were determined to be early stage and other nine were advanced-stage using histopathological analyses. All early-stage and advanced-stage OPA cases showed positive labelling for JSRV CA, Ki67, COX-1, and COX-2. COX-1, COX-2 and Ki67 immunopositivity levels were found to be statistically higher in advanced-stage OPA compared to early-stage OPA. In Western blot analyses, COX-1 and COX-2 expression levels were found to be higher in advanced-stage OPA infections compared to early-stage OPA infections. It was therefore concluded that chronic inflammation and alveolar macrophages could contribute to the development of OPA. Similar to lung cancer in humans, the use of COX inhibitors for the treatment of OPA is thought to be highly effective.

To Cite This Article: Bozkurt MF, Karakurt E, Zafar M, Bolat I, Çomakli S, Coşkun N, Bolat M, Yildirim S, Beytut E, Kiziltepe S, Yilmaz V, Kiliçlioğlu M, Korkulu E and Özbay YT, 2026. Cyclooxygenase-1 & -2 and Ki67 expression in early- and advanced-stage ovine pulmonary adenocarcinomas. Pak Vet J, 46(7): 1722-1731. http://dx.doi.org/10.29261/pakvetj/2026.165

INTRODUCTION

Ovine pulmonary adenocarcinoma (OPA), or Jaagsiekte, previously known as pulmonary adenomatosis, is a progressively worsening disease. It is known for being a contagious neoplastic pulmonary disease of viral origin, although most commonly seen in sheep, but has also been reported, albeit rarely, in goats and small ruminants such as wild sheep (Toma *et al.*, 2025; Hodor *et al.*, 2026). This disease results from Jaagsiekte sheep retrovirus (JSRV) (exogenous form, exJSRV) infection and is transmitted from one animal to another, mostly through the inhalation of viral particles (Ortega *et al.*, 2023; Coskun *et al.*, 2024; Cousens *et al.*, 2024). In addition, the virus has been detected in milk and colostrum (Scott *et al.*, 2018). JSRV mainly infects type 2 pneumocytes and non-ciliated

bronchial club cells, causing the neoplastic transformation of these cells (Cousens *et al.*, 2015; Quintas *et al.*, 2021). Thus, the tumor growths formed by these cells spread into the alveolar septa and bronchioles. JSRV virions are propagated in infected cells and these virions spread through the lung, creating new locations of infection and neoplastic areas, leading to a progressive tumor onset (Youssef *et al.*, 2015).

OPA has been reported in many countries across America, Asia, Africa, European regions, Australia, New Zealand, the Falkland Islands, and Iceland (Lee *et al.*, 2017; Chen *et al.*, 2024). The lack of an effective vaccine or therapeutic drug against this disease means that OPA continues to place a constant economic burden on the global sheep industry (Du and Liu, 2026). For these reasons, the World Organization for Animal Health (WOAH) classifies OPA as a significant infectious disease (Zhang *et al.*, 2025).

Besides the importance in veterinary field, OPA is quite similar to various human lung adenocarcinomas, such as non-small-cell lung cancer, the resemblance is due to histological features and similar common cell signaling pathway activation. For this reason, it is regarded as a good model for explaining the mechanisms of pulmonary carcinogenesis (Sun *et al.*, 2017; Zhang *et al.*, 2024; Toma *et al.*, 2025).

Tumor progression is critically dependent on the tumor stroma and tumor microenvironment (TME). The TME includes inflammatory, regenerative, and immune cells, as well as the cytokines and mediators they secrete. Some of the cytokines and mediators secreted by cells in the TME play a tumor-suppressive role, whereas others promote tumor development (Carvalho *et al.*, 2018). Cyclooxygenase (COX), an enzyme belonging to the myeloperoxidase family, can catalyze arachidonic acid into proteinoids. These include prostaglandins, thromboxane, and prostacyclin, which are biologically active proteins that can regulate various physiological processes in both animals and humans. There are three isoforms of COX: COX-1, COX-2, and COX-3. COX-1 is detected in normal tissues and organs while COX-3 is mainly expressed in the aortic wall and central nervous system (Xinyi *et al.*, 2025). Cyclooxygenase-2 (COX-2) is known for its role in synthesis of proteinoids, which are key mediators of inflammation and pain. Like cyclooxygenase-1, COX-2 expression is increased in response to various stimuli, like effect of hormones, inflammatory cytokines, growth factors, and oncogenes (Diop *et al.*, 2025). The overexpression of COX enzymes is associated with poor prognosis in many types of cancer, including histological type, recurrence, and regional lymph node metastasis, in both human and veterinary medicine (Vieira *et al.*, 2022; Wojtkowska *et al.*, 2024).

Studies report cyclooxygenase expression in some cat and dog tumors and also in equine tumors (Doré, 2011). However, no literature data evaluating cyclooxygenase levels in OPA has been identified. Therefore, in this study, COX-1 and COX-2 expression in the early and advanced stages of OPA was evaluated using immunohistochemistry and Western blotting. In addition, the proliferation index was assessed using Ki67 expression. The aim was to determine whether there was any connection between the development of OPA and cyclooxygenase levels.

MATERIALS AND METHODS

Animals and Clinical Findings: 18 lung tissue samples were taken from the Pak Food Meat Integrated Facility (Local Company) in 2026 and were used as study material. Animals were chosen for the disease-specific symptoms and macroscopic lesions. Ten of the animals were male and eight were female. The animal breeds were Morkaraman and Crossbreeds. Their average age was 3.5 years. Animal owners were asked for the anamnesis information prior to slaughter at the abattoir, the animals showed clinical signs such as severe coughing, breathing difficulties, nasal discharge, weakness, and separation from the herd. Two healthy sheep lung tissues were used as negative control.

Ethics Committee Report: This study's design was in line with the Local Ethics Committee for Animal Experiments of Kafkas University (Number: KAU-HADYEK-2025/259, Acceptance Date: 26.12.2025).

Tissue homogenization: Tissues were processed individually. Approximately 1g of tissue was collected from the lungs of 18 sheep (9 early-stage and 9 advanced-stage). The tissues were homogenized using a mortar and pestle. The homogenates were placed into polystyrene tubes. Phosphate buffered saline (PBS) was used as the diluent. 900ml of PBS were added to each tube before vortexing for 5min. The tubes were centrifuged at 3000rpm for 10min. The supernatants were carried over to new tubes and stored at -20°C for nucleic acid extraction.

Nucleic acid extraction: The HighPure Viral Nucleic Acid Extraction Kit (Cat: 11858874001, Roche, Germany) was used for viral nucleic acid purification according to the manufacturer's instructions. Extracts were stored at deepfreeze (-20°C) before molecular studies.

One-Step Reverse Transcription Polymerase Chain Reaction (RT-PCR): OPA is caused by the exogenous form of Jaagsiekte Sheep Retrovirus (exJSRV), which has an RNA genome. Since endogenous and exogenous forms are quite similar at the molecular level, a primer pair targeting the U3 region, designed by Palmarini *et al.* (1996), was used. The primer pair P1-P3 was used in a single-step PCR, but since exJSRV has an RNA genome, an initial reverse transcription (RT) step was required. RT and PCR were both performed using the 2X One-step RT-PCR kit from Hibrigen (Turkey, Catalogue Number: MG-OSPM-01). The thermal cycler conditions were applied as described in the referenced publication. An exJSRV positive extract from previous studies was used as a positive control. Molecular-grade distilled water was used for the negative control. The amplicons were visualized in a 1% agarose gel (Cat: MG-AGRZ-01-100, Hibrigen, Turkey) with SafeView™ DNA Stains (Cat No: G108-R, Applied Biological Materials, Richmond, BC, Canada) using a UV transilluminator (MIULAB UV-6, Hangzhou, China). The expected positive amplicon size was approximately 176bp.

Histopathological Examinations: Lung tissues belonging to sheep were fixed in a 10% formaldehyde solution. Routine tissue processing steps were followed; serial

sections of each 5 micrometers were cut from the paraffine blocks. Sections were stained with Haematoxylin & Eosin (H&E) to evaluate histopathological changes. Light microscope was used to investigate the changes by two different pathologists. Noteworthy pathological findings (reproduction patterns, tumor microenvironment, inflammatory infiltration) were recorded for each case and photographed at different magnifications (Karakurt *et al.*, 2023).

Immunohistochemical Examinations: Four micrometers thick serial sections were cut from paraffin blocks prepared from samples. Staining of JSRV capsid protein (JSRV CA), COX-1, COX-2, and Ki67, with commercial antibodies were performed using Avidin-Biotin Peroxidase Technique (ABC) in line with the manufacturer's procedures were stained using. Information on staining technique used in this study is provided in Table 1. Thermo Scientific Histostain IHC Kit (HRP, broadspectrum, REF: TP-125-HL) was used for the immunostaining procedures. To reveal the reactions as chomogenic substrates, Aminoethylcarbazole (AEC, Thermo Scientific, REF: TA-125-HA) and 3,3'-diaminobenzidine (DAB, Thermo Scientific, REF: TA-125-HD) were applied for ~15min. Sections were rinsed with tap water for 5min and then Mayer's Haematoxylin stain was applied for 1min. If AEC chromogen was used sections were rinsed in distilled water and then covered with the AEC mount. If DAB chromogen was used sections were passed through alcohols of increasing concentration and xylene, then mounted with Entellan and evaluated under a light microscope (Olympus Bx53). Cell^P software (Olympus Soft Imaging Solutions GmbH) was used for taking the photographs of the sections. Detailed analysis of the photographs were performed using the ImageJ software (v1.51j8). (Karakurt *et al.*, 2025).

Table 1: Information on primary antibodies used in immunohistochemical examinations

Primary Antibodies	Company, Clone and Catalogue Numbers	Pre-treatment	Dilution	Incubation Conditions
JSRV CA	Supplied by Prof. Massimo Palmarini, polyclonal	Microwave oven	1/1500	Overnight, 4 °C
Ki67	Epredia, Monoclonal, Cat no: RM-9106	Microwave oven	1/100	Overnight, 4 °C
COX-1	Santa Cruz Biotechnology, Monoclonal, Cat no: sc-19998	Microwave oven	1/100	Overnight, 4 °C
COX-2	Abcam, Polyclonal, Cat no: ab15191	Microwave oven	1/100	Overnight, 4 °C

Immunohistochemical staining results were analyzed using a grading system that was based counting the number of positive cells in immune-positive areas. The quantification of immune-positive reactions in tissues was initiated by analyzing areas with high-intensity reactions. In each case, tumor tissue was observed and three different areas were selected and evaluated using a 50× objective lens. Tumor cells and inflammatory cells which were positive in the tumor microenvironment was counted separately. Average of these three areas was noted as the grade of the OPA case. Grading was recorded as: (-) no immunoreactivity; (+) weak, 1-10% positivity; (++) moderate, 11-59% positivity; and (+++) intense, >60% positivity (Karakurt *et al.*, 2022c).

Statistical Analysis: Shapiro–Wilk test was selected for the normalizing of the data distribution. The independent samples Student's t-test was used to compare immunohistochemical data showing a normal distribution between two independent groups. GraphPad Prism software used for all statistical analyses, and data were evaluated considering $P<0.05$ as statistically significant (Bolat *et al.*, 2026).

Western Blot: RIPA lysis buffer (sc-24948, Santa Cruz Biotechnology, Inc., Texas, USA) was added to the tissue homogenates, and the tissues were homogenized to obtain supernatants. BCA Protein Assay Kit (Rockford, IL, USA) was used for quantifying protein. Separation of proteins were achieved using 10% SDS-polyacrylamide gels (SDS-PAGE). The proteins were transferred to polyvinylidene difluoride (PVDF) membranes using a semi-dry blotting system (Thermo, Rockford, IL, USA). Following blocking, overnight incubation of the membranes at 4°C was performed using primary antibodies (diluted in TBS-T): β-tubulin (sc-47778), COX-1 (sc-20067), and COX-2 (sc-7382). A second incubation for 1.5h with goat anti-mouse IgG-HRP secondary antibody (sc-2005, Santa Cruz Biotechnology, Inc., Texas, USA) was performed with a 1:1000 dilution at room temperature. Visualization of the bands was done using Trident Femto Western HRP Substrate (GeneTex GTX14698). GelDoc XR imaging system (Bio-Rad, USA) was used for capturing images and Image Lab 6.1 software (Bio-Rad, USA) was used to measure protein expression analysing band intensities. This analysis was repeated three times (Bolat *et al.*, 2026).

RESULTS

Macroscopic Findings: In early-stage OPA-affected lungs, diaphragmatic lobes were the place where lesions were predominantly observed. The lesions had different sizes and were demarcation of these lesions from the surrounding normal tissue was definite. The lesions were mostly greyish-white. The majority of cases presented a solitary structure. Multifocal nodular tumor foci were less common. The consistency of the tumor foci was quite firm, and their cut surfaces were relatively dry and lacking exudate (Fig. 1A).

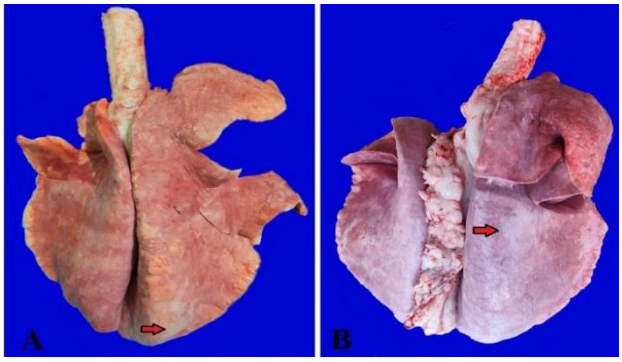

Fig. 1: A: Early-stage OPA, **B:** Advanced-stage OPA, Macroscopic appearance of tumor foci (red arrows).

Compared to early-stage OPA cases, lesions in advanced-stage OPA were not concentrated in a distinct lobe. Tumor areas were seen in the caudal, medial, and cranial lobes. These tumor areas varied in color (greyish-white and pinkish). Compared to early-stage OPA, the tumor foci were not clearly demarcated from the surrounding normal tissue and had an irregular shape. These foci had firm consistencies. Some cases showed a tendency for neoplastic areas of varying sizes to coalesce. Moreover, in some cases, the lesions were such severe that it eliminated a significant portion or almost the entire lobe of the lung. Compared to early-stage OPAs, the cross-sectional surfaces of the tumor foci were considerably moist (Fig. 1 B).

Molecular Findings: Exogenous Jaagsieskte Sheep Retrovirus RNA was detected in all samples. Results of the One-step RT-PCR are shown in Fig. 2 A and B. All samples yielded a 176 bp product, indicative of exJSRV RNA (Fig. 2).

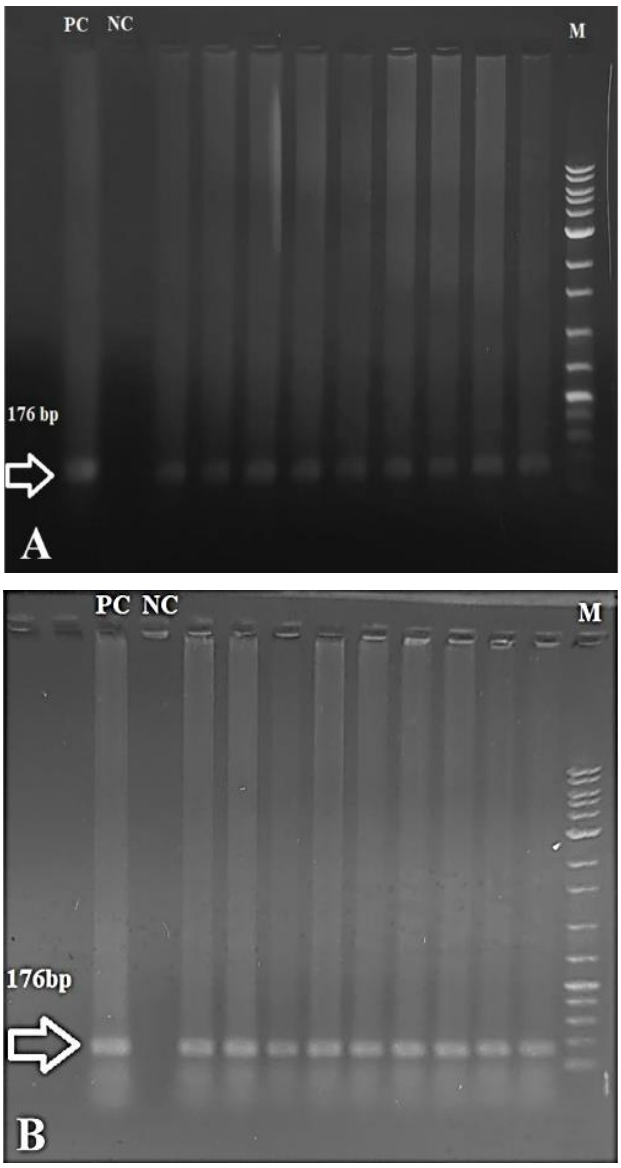

Fig. 2: Gel image of One-step RT-PCR results of early-stage **(A)** and advanced-stage **(B)** samples. PC: Positive control, NC: Negative control, M: Marker. Wells contain amplicons of 9 samples, each amplicon has a 176 bp product, indicating nucleic acid presence.

Histopathological Findings: Cancer development patterns in early- and advanced-stage OPA are shown in Table 2. In early-stage OPA, the tumor foci were observed to be considerably small and few. However, it was noted that these tumor foci were distinctly separated from the surrounding normal lung tissue (Fig. 3). In advanced-stage cases, such separation was not present. The tumor foci had completely infiltrated the lung tissue. It had a highly aggressive spread (Fig. 4). Regardless of the stage, neoplastic cells were observed to be columnar or cuboidal in all cases. The degree of differentiation of the neoplastic cells was good. The pleomorphism was quite moderate. Although not very remarkable, mitotic figures were observed in some areas. Within the alveolar lumens and bronchioles, the tumor cells mostly exhibited papillary and acinar growth patterns. Papillary formations were predominant in some areas, a pattern that was most prominent in early-stage cases. In some cases, acinar formations were dominantly observed. Additionally, papillary and acinar growth patterns were most often observed together. In addition to these cancer development patterns, fibromyxoid proliferations were detected in two advanced-stage cases, and lepidic proliferations were observed in one case. Tumour-cell clusters within the bronchioles and alveoli, sometimes quite small and sometimes reaching enormous sizes, were particularly remarkable. The stromal tissue surrounding the alveoli and bronchioles was considerably thickened due to an increase in mononuclear cells and connective tissue. There was a very intense inflammatory cell infiltration around the tumor foci. Alveolar macrophages predominantly dominated the tumor microenvironment. Severe lymphoid hyperplasia, parasitic pneumonia, neutrophil infiltration and necrotic foci that could reach quite large sizes were noteworthy histopathological findings seen in advanced-stage OPA. The secondary infection appearance was much milder in early-stage OPA (Fig. 5).

Table 2: Cancer growth patterns of all OPAs

Case	Stage	Pattern
1	Early	Papillary
2	Early	Papillary
3	Early	Papillary
4	Early	Papillary
5	Early	Papillary
6	Early	Papillary + Acinar
7	Early	Papillary
8	Early	Papillary
9	Early	Papillary + Acinar
10	Advanced	Papillary + Acinar
12	Advanced	Papillary + Acinar
13	Advanced	Papillary
14	Advanced	Acinar
15	Advanced	Papillary + Acinar + Fibromyxoid
16	Advanced	Papillary + Acinar + Lepidic
17	Advanced	Papillary + Acinar + Fibromyxoid
18	Advanced	Papillary + Acinar

Immunohistochemical Findings: All early-stage and advanced-stage OPA cases showed positive staining for JSRV CA, Ki67, COX-1, and COX-2. JSRV CA immune-positive reactions were concentrated in the cytoplasm (membranous) of the neoplastic cells forming papillary and acinar structures. There was no significant difference in the JSRV CA expression between papillary, acinar,

fibromyxoid, or lepidic growth patterns. Ki67-positive staining was predominantly detected in the nuclei of cells in the stromal tissue in both early and advanced OPA. In advanced cases, intranuclear staining was present in papillary and acinar structures, as well as in the stroma, albeit to a lesser extent. Although rare, mitotic figures were observed to be positive for Ki67 immunoreactivity. It was noteworthy that the reaction was much more intense in tumor-support cells than in tumor cells (Fig. 6). COX-1 and COX-2 reactions were detected in the cytoplasm of tumor cells and determined as positive, especially reactions located in papillary and glandular structures protruding into the alveolar lumen. Besides these papillary and acinar formations, positive staining was also observed in tumor cell clusters of varying numbers and sizes within the alveoli and bronchioles. Similarly, dark brown COX-1 and COX-2 expression within the cytoplasm were observed in alveolar macrophages in the tumor microenvironment. Similarly, the tumor stroma was also found to be positive for these two biomarkers. COX-1 and COX-2 expressions were much more intense in papillary proliferations than in acinar proliferations. The most intense reactions in early and advanced stages of OPA were predominantly detected in papillary formations. Although not at a significant intensity, cyclooxygenase immunoreactivity was also detected in tumor areas exhibiting both fibromyxoid and lepidic patterns (Fig. 7). In conclusion, COX-1 ($P<0.0001$), COX-2 ($P<0.0001$) and Ki67 ($p=0.0001$) immunopositivity levels were found to be statistically higher in advanced-stage OPA compared to early-stage OPA (Fig. 8).

Western Blot Findings: In lung samples, COX-1 ($P<0.0001$) and COX-2 ($p=0.0016$) expression levels were found to be higher in advanced-stage OPA infections compared to early-stage OPA infections. The image obtained from Western blot tests are shown in duplicate in Fig. 9A. The statistical analysis data for the values obtained from the bands are presented in Fig. 9B for COX-1 and Fig. 9C for COX-2.

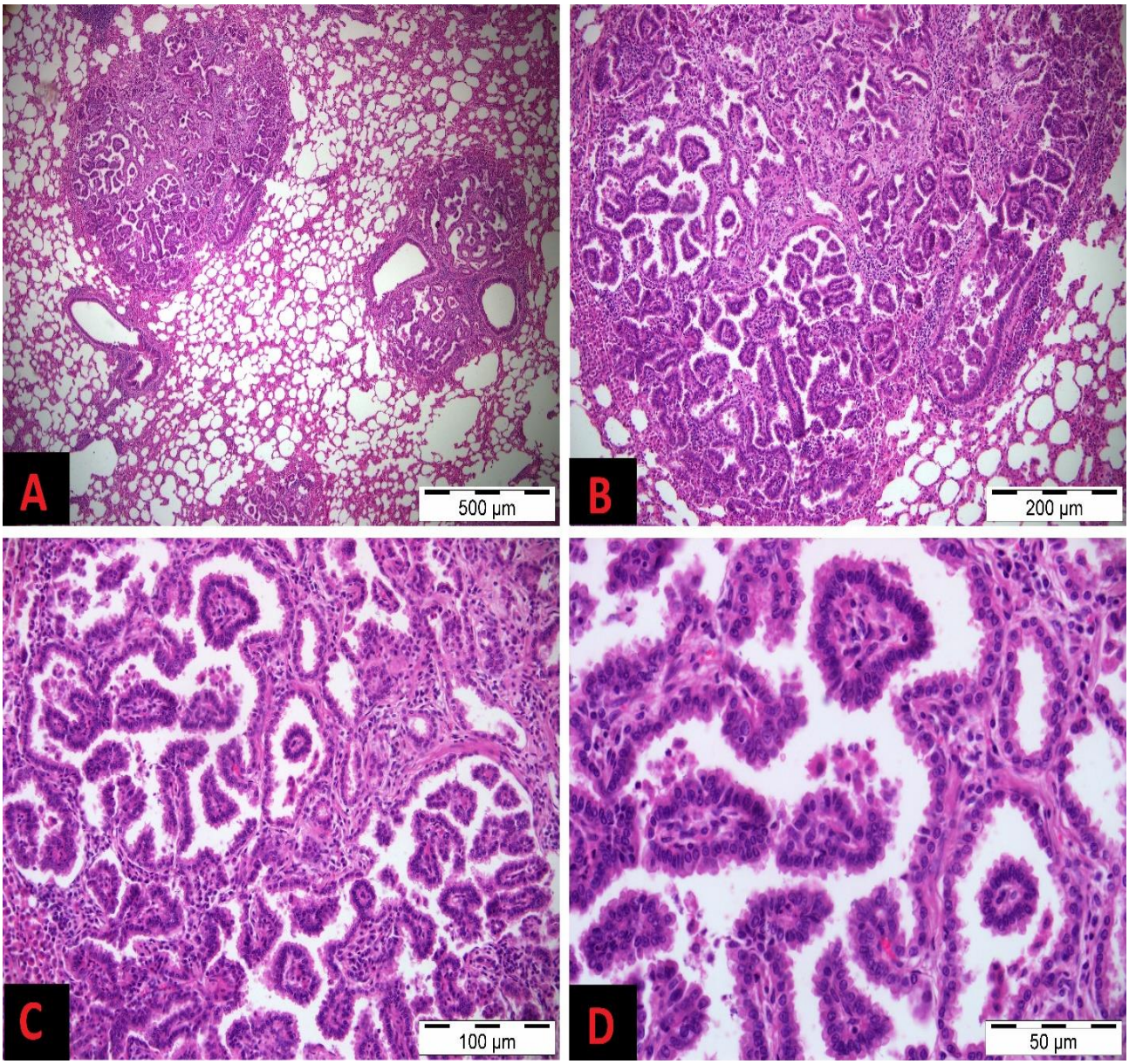

Fig. 3: Sheep lung, early-stage OPA, A-B: oval-shaped tumoral foci of varying sizes, diffusely distributed throughout the lung parenchyma, shown at different magnifications, C-D: Tumoral masses and papillary structures within the alveolar lumen, shown at different magnifications, H&E.

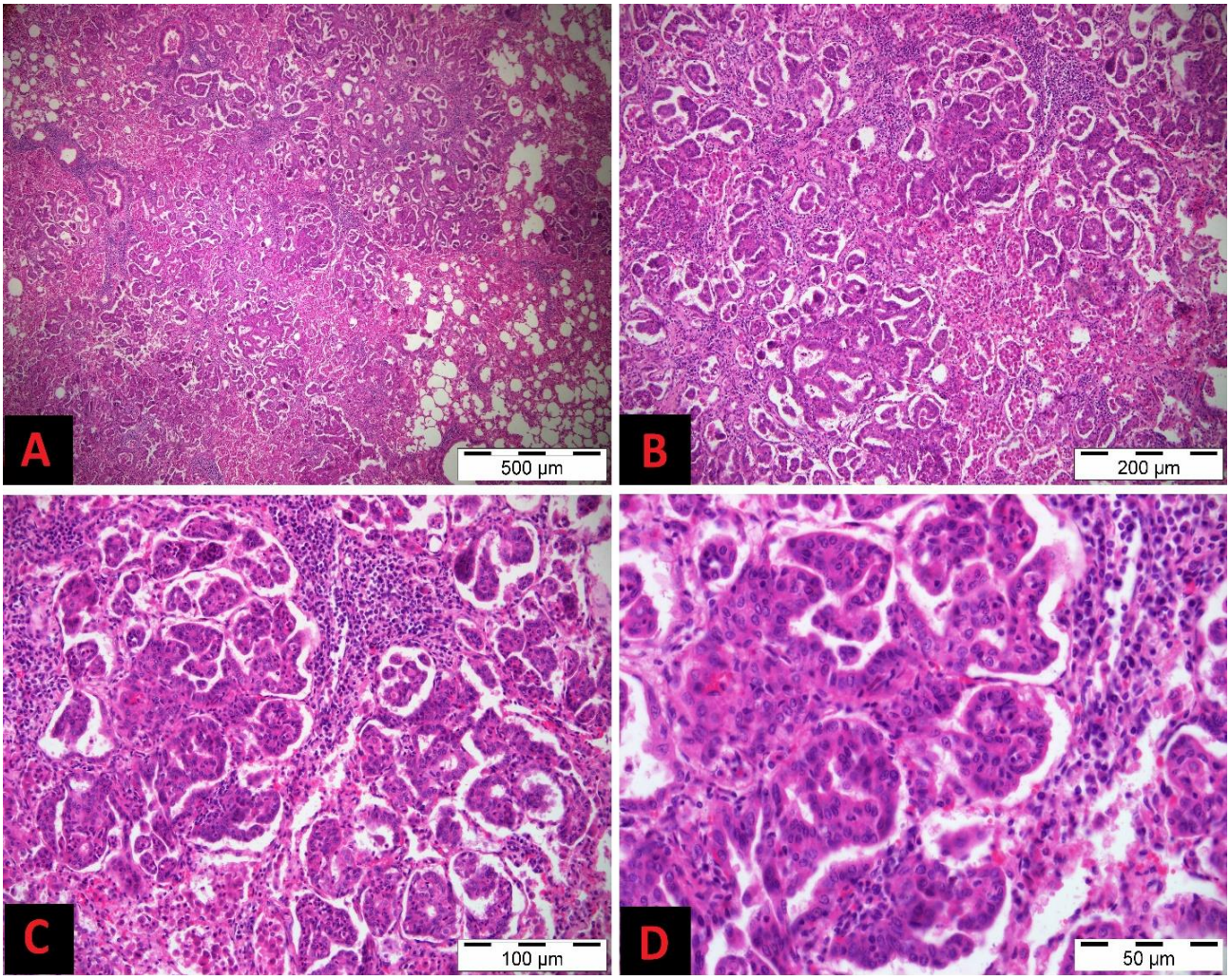

Fig. 4: Sheep, lung, advanced-stage OPA, A-B: Widespread proliferative lesions in the lung parenchyma at different magnifications, C–D: Acinar type proliferations within the alveolar spaces at different magnifications, H&E.

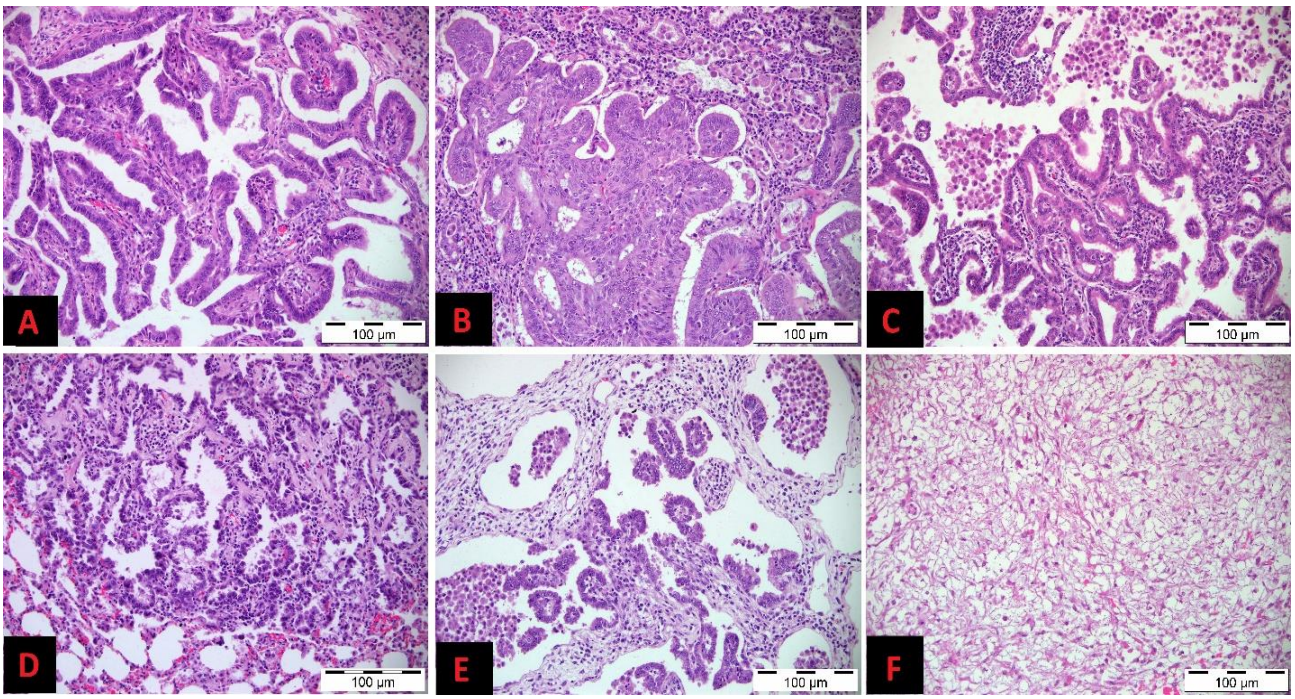

Fig. 5: Sheep, lung, cancer patterns, **A:** Papillary pattern, **B:** Acinar pattern, **C:** Mixed pattern, **D:** Lepidic pattern, **E:** Tumour-cell clusters and surrounding alveolar macrophages, **F:** Fibromyxoid pattern.

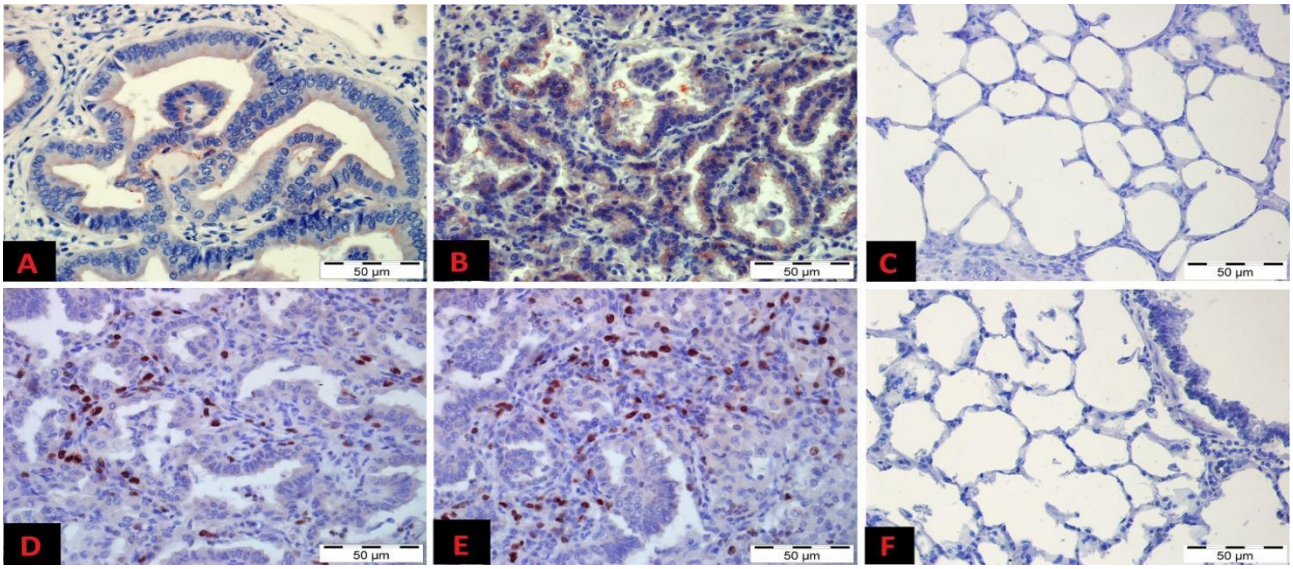

Fig. 6: Sheep, lung, JSRV CA (A-B-C) and Ki67 (D-E-F), IHC, AEC, **A:** Early-stage OPA, JSRV CA membranous positive labelling in the tumoral cells, **B:** Advanced-stage OPA, intracytoplasmic JSRV CA expression in neoplastic cells, **C:** Negative control, JSRV CA, **D:** Early-stage OPA, intranuclear positive labelling in the tumoral stroma and mitotic figures, **E:** Advanced-stage OPA, dark red, highly intense reactions in the tumoral stroma and the nuclei of neoplastic cells, F: Negative control.

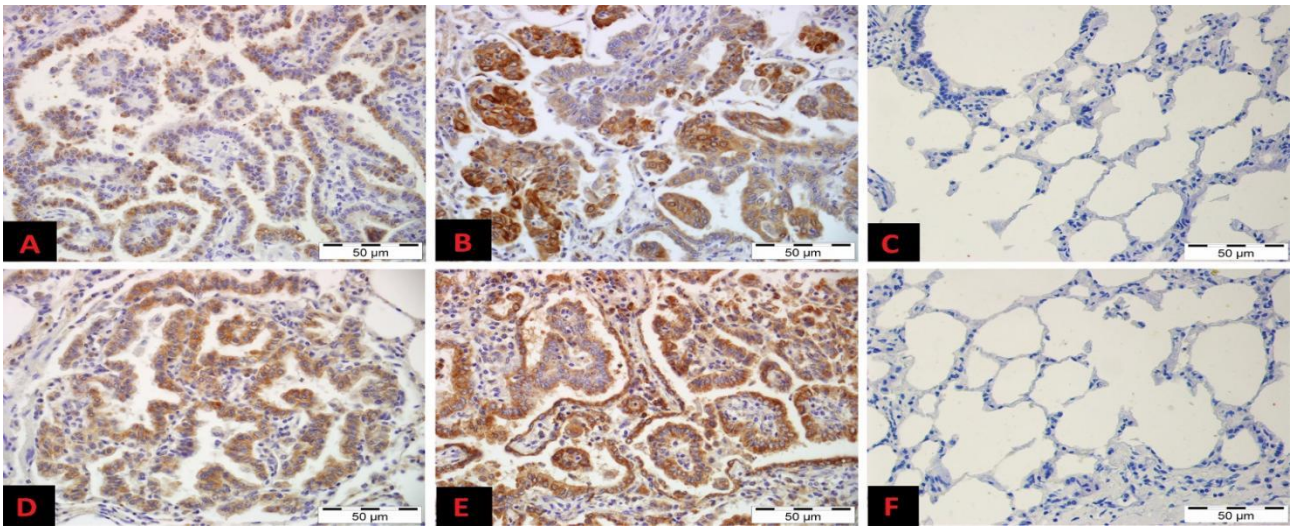

Fig. 7: Sheep, lung, COX-1 (A-B-C) and COX-2 (D-E-F), IHC, DAB, **A:** Early-stage OPA, Mild intracytoplasmic positive reactions in neoplastic cells forming finger-like extensions and in tumoral cell masses, **B:** Advanced-stage OPA, Highly intense cytoplasmic labeling in tumoral masses and papillary structures within alveolar lumens, **C:** Negative control, **D:** Early-stage OPA, Cytoplasmic expressions in papillary structures within a small, well-demarcated tumoral focus, **E:** Advanced-stage OPA, Intracytoplasmic dark brown positive reactions in alveolar macrophages, tumoral cell masses, and papillary formations, **F:** Negative control.

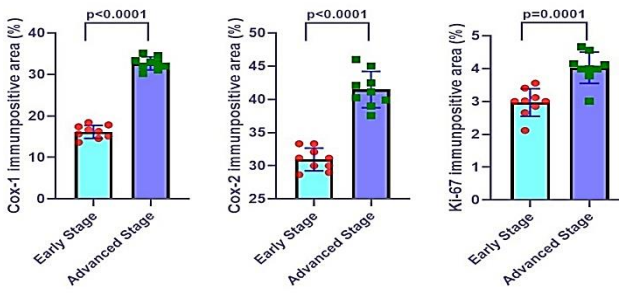

Fig. 8: Comparison of COX-1, COX-2, and Ki67 immuno-positive area percentages in early and advanced stage groups. Images obtained after immunohistochemical staining were analyzed using ImageJ software and quantitatively evaluated as immune-positive area (%). Data are presented as mean ± SD. Statistical comparisons between two independent groups were performed using the independent samples Student's t-test, and a $p<0.05$ value was considered statistically significant.

DISCUSSION

This disease shows no gender or breed predisposition (Toma *et al.*, 2020). It mostly affects sheep aged 2 to 4 years. The most prominent clinical signs of this disease are profuse, frothy nasal discharge, dyspnoea, and weight loss (Reséndiz-Pozos *et al.*, 2025). In addition to tumor lesions, various bacterial agents (such as *Mannheimia* and *Mycoplasma*), viral (Maedi-Visna) and parasitic pneumonias can aggravate the clinical picture (Quintas *et al.*, 2021). In this study, consistent with the literature, tumor lesions were found in study sample pool which includes different breeds, males and females with an average age of 3.5 years. However, in the current study, the clinical findings were much more severe and showed greater variability in advanced-stage OPA than in early-

stage OPA. In early-stage cases, there were no noteworthy clinical findings based on the anamnesis provided by the owners. However, histopathological examinations revealed that secondary infections were much more prevalent in advanced-stage cases compared to early-stage cases. The most prominent secondary infection was severe bronchopneumonia. In addition, parasitic pneumonia and severe lymphoid hyperplasia, indicative of Maedi infection, also accompanied OPA cases.

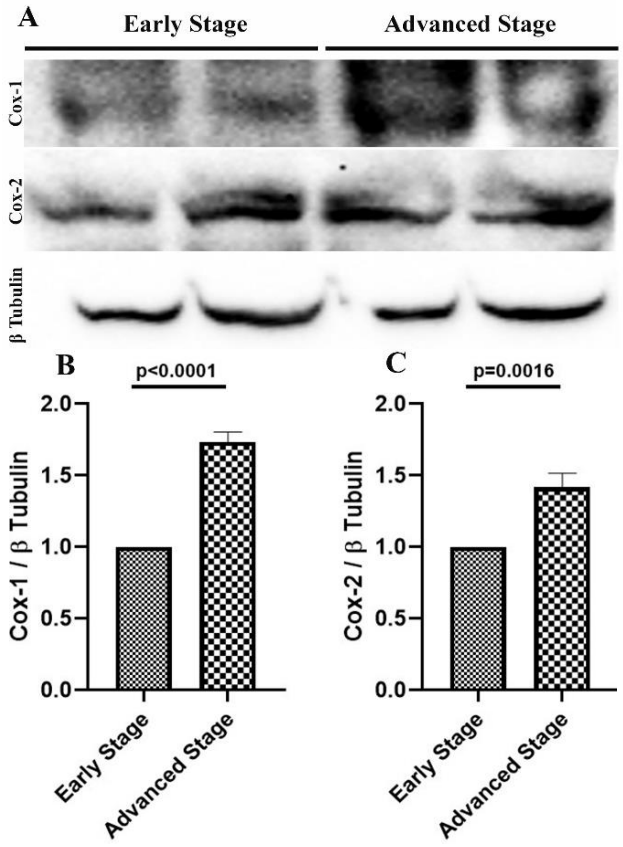

Fig. 9: Protein bands from Western blot analyses performed on lung tissues in early and advanced stages of OPA infection, and statistical analysis data for these bands. **A:** Protein bands obtained from Western blot analyses. Images of two replicate bands for each stage are presented. **B:** Statistical analysis result for COX-1. **C:** Statistical analysis results for COX-2. One-way ANOVA followed by Tukey's test was performed for the statistical analysis of the data. Data are presented as mean±SD.

Laboratory tests are limited because the host fails to mount a detectable antibody response to JSRV infection (Hodor *et al.*, 2026). Unfortunately, no treatment or vaccine has been developed for this infection (Scott *et al.*, 2018). In this study, 18 lung tissue samples suspected of OPA based on macroscopic pathology data were collected from the slaughterhouse. Following histopathological examination, OPA was diagnosed in the tumor masses. This diagnosis was supported by both molecular and immunohistochemical methods.

This disease was previously defined as pulmonary adenomatosis due to its non-invasive nature (Youssef *et al.*, 2015). However, due to the presence of intrathoracic and extra-thoracic metastases in 10% of the cases, OPA is now classified as a malignant disease (Minguijón *et al.*, 2013; Hodor *et al.*, 2026). In the current study, both advanced and early-stage OPA cases were thoroughly examined for the presence of metastases in regional lymph nodes or distant organs such as the liver, kidneys, and spleen. However, consistent with the literature data (Karakurt *et al.*, 2022d), no tumor foci were detected in the aforementioned lymph nodes or organs.

Ki67 is a nuclear protein which is being expressed during active phases of the cell cycle and is largely used as an immunohistochemical marker to assess the cellular proliferation index (Reséndiz-Pozos *et al.*, 2025). In this study, Ki67 immuno-positive reactions were significantly increased in advanced-stage OPA compared to early-stage OPA. However, Ki67-positive staining was rather mild in both stages. Ki67 immunoreactivity was present not only in tumor proliferations but also in the tumor stroma. The areas with the most intense reactions were those with papillary pattern rather than an acinar, lepidic, or fibromuscular pattern. Consistent with the literature (De las Heras *et al.*, 2014; Toma *et al.*, 2020; Reséndiz-Pozos *et al.*, 2025; Hodor *et al.*, 2026), few staining were detected in mitotic figures. Although classified as a malignant tumor, the Ki67 immunohistochemical findings from the current study indicate that OPA has a very low proliferation index.

The tumor microenvironment (TME) encompasses all components that interact with cancer cells. This environment is characterized by the upregulation of pro-inflammatory mediators such as cyclooxygenase (COX) enzymes. COX-1 and COX-2 play a role in regulating the immune response and may contribute to angiogenesis, cancer cell proliferation and motility, and inhibition of apoptosis (Musser *et al.*, 2025). COX-1, which is responsible for various physiological activities, can be detected in normal tissues and organs, whereas COX-2 is not. In this study, COX-1-positive staining was detected in tumor foci as well as in the surrounding healthy areas, whereas COX-2-positive staining was much more specific than COX-1 and was cancer-centred rather than in normal areas. This data confirms COX-2's relationship with more aggressive cancer subtypes and validates COX-2 as a highly useful prognostic biomarker (Brandi *et al.*, 2023). In cancer formation, COX-2 is primarily active in the tumor microenvironment. It exhibits anti-apoptotic features by B-cell lymphoma 2 inhibition, producing vascular endothelial growth factor (VEGF) to increase angiogenesis, supporting vascular budding, migration, and tube formation. And it also influences epidermal growth factor (EGF) activation, and matrix metalloproteinases induction. Previous studies (Karakurt *et al.*, 2022a, Karakurt *et al.*, 2022b, Karakurt *et al.*, 2022c Karakurt *et al.*, 2023, Karakurt *et al.*, 2025) have reported that the severity of inflammation in the tumor microenvironment, cytokine levels, and growth factors play a critical role in OPA development. The current study found COX-1 and COX-2 immuno-positive staining in tumor cells and inflammatory infiltrates in the tumor microenvironment, particularly in alveolar macrophages, at both the early and advanced stages of OPA. The intensity of cyclooxygenase staining was significantly increased in areas where the inflammatory reaction was heightened. This immunohistochemical finding from the study also supported the proinflammatory properties of cyclooxygenases (Santelices Iglesias *et al.*, 2018). Particularly in advanced-stage cases, inflammatory cell infiltration in the tumor microenvironment, especially the presence of alveolar macrophages, was much more severe

than in early-stage cases. Inflammatory infiltration was equally intense in parallel with the increase in tumor burden. However, the significant increase in cyclooxygenase expression in advanced-stage OPA compared with early-stage OPA indicates that cyclooxygenases play a key role in cancer development.

Chronic inflammation causes the release of proinflammatory mediators such as prostaglandins, cytokines, and chemokines from stromal cells, transforming the tissue microenvironment from normal to abnormal (Carvalho *et al.*, 2016; Carvalho *et al.*, 2017). In this type of lung cancer in sheep, which has a viral etiology and a long incubation period, viruses trigger chronic inflammation, which upregulates cyclooxygenase enzymes. A direct relationship has been found between cyclooxygenase levels and cancer aggressiveness. In particular, alveolar macrophage infiltration, which is highly characteristic of OPA, appears to play an active role in OPA progression. Compared with early-stage cases, advanced-stage cases had more secondary infections, including vermiform pneumonia, Maedi, and bronchopneumonia, in addition to OPA lesions. This has been interpreted as indicating that not only alveolar macrophage infiltration but also different types of inflammatory responses accompanying tumor lesions contribute to the cancer process. Furthermore, a positive correlation was found between the severity and duration of inflammatory infiltration and cancer aggressiveness. It was demonstrated that not only inflammatory infiltration in the TME but also stromal cells in the tumor contribute to tumor development, as evidenced by both Ki67 and cyclooxygenase immune-positive staining.

OPA exhibits many similarities to human lung cancers, including histological appearance and signaling pathways. In this regard, we believe that the data obtained from the current study will contribute to the veterinary and medical literature by clarifying aspects of viral oncogenesis. Based on data from the current study, the use of cyclooxygenase inhibitors for therapeutic purposes holds significant potential in reversing the disease, as there is still no effective treatment, vaccine, or diagnostic kit available for OPA. Lung cancers account for a significant proportion of cancer-related deaths in humans. COX-2 inhibitors, which are used in the treatment of breast, prostate, colon, and lung cancers, particularly non-small-cell lung cancer, and are known to be successful in cancer regression, may be quite useful in regressing OPA lesions in this regard (Liu *et al.*, 2015; Pu *et al.*, 2021; Liu *et al.*, 2024).

Conclusions: The data obtained from the current study can be summarized as follows. Firstly, it was observed that COX expression increased significantly in parallel with tumor burden in OPA. In addition, it was demonstrated that COX, particularly COX-2, is associated with a poor prognosis for OPA. COX immunoreactivity was detected intensely not only in papillary, acinar, lepidic, fibromyxoid, or tumor-cell clusters but also in the TME. In this regard, it was concluded that chronic inflammation and alveolar macrophages also contribute to the development of OPA. Finally, it is thought that, similarly to lung cancer in humans, the use of COX inhibitors for the treatment of OPA would be highly effective.

Authors Contribution: MFB, EKa, MZ and NC concept, idea, writing, YTÖ and MK histopathology and immunohistochemistry, IB and MB western blot analyses, NC, VY and Eko molecular analyses, MFB, EKa, EB, SÇ and SY histopathological and immunohistochemical analyses, ŞK clinical analyses

Financial Support: The authors declare that this study has received no financial support.

Acknowledgement: We would like to express our gratitude to Professor Massimo Palmarini (Institute of Comparative Medicine, Faculty of Veterinary Medicine, University of Glasgow, UK) for providing the rabbit anti-JSRV CA primary antibody.

Conflict of Interest: The authors declared that there is no conflict of interest.

REFERENCES

Bolat İ, Beytut E, Sağlam YS, *et al.*, 2026. Maedi infection modulates oncogenic and inflammatory signaling in ovine pulmonary adenomatosis through TLR4/NF-κB and JAK2/STAT3 pathways: A Trojan horse mechanism. Veterinary Microbiology 314:110906.

Brandi A, de Faria Lainetti P, Elias F, *et al.*, 2023. Firocoxib as a potential neoadjuvant treatment in canine patients with triple-negative mammary gland tumors. Animals (Basel) 13:60.

Carvalho MI, Pires I, Prada J, *et al.*, 2017. High COX-2 expression is associated with increased angiogenesis, proliferation and tumoural inflammatory infiltrate in canine malignant mammary tumours: a multivariate survival study. Veterinary and Comparative Oncology 15:619-631.

Carvalho MI, Silva-Carvalho R, Pires I, et al., 2016. A comparative approach of tumor-associated inflammation in mammary cancer between humans and dogs. BioMed Research International 2016:4917387.

Carvalho MI, Bianchini R, Fazekas-Singer J, *et al.*, 2018. Bidirectional regulation of COX-2 expression between cancer cells and macrophages. Anticancer Research 38:2811-2817.

Chen S, Zhang P, Duan X, *et al.*, 2024. Lesion localization and pathological diagnosis of ovine pulmonary adenocarcinoma based on MASK R-CNN. Animals (Basel) 14:2488.

Coskun N, Yilmaz V, Karakurt E, *et al.*, 2024. Molecular and pathological detection of Jaagsiekte sheep retrovirus in lung tissues of sheep. Kafkas Universitesi Veteriner Fakultesi Dergisi 30:809-814.

Cousens C, Alleaume C, Bijsmans E, *et al.*, 2015. Jaagsiekte sheep retrovirus infection of lung slice cultures. Retrovirology 12:31.

Cousens C, Meehan J, Collie D, *et al.*, 2024. Tracking ovine pulmonary adenocarcinoma development using an experimental Jaagsiekte Sheep Retrovirus infection model. Genes (Basel) 15:1019.

De las Heras M, de Martino A, Borobia M, *et al.*, 2014. Solitary tumours associated with Jaagsiekte retrovirus in sheep are heterogeneous and contain cells expressing markers identifying progenitor cells in lung repair. Journal of Comparative Pathology 150:138-147.

Diop N, Canonne AM, Huet H, *et al.*, 2025. Immunohistochemical evaluation of cyclooxygenase-2 expression in feline nasal malignant epithelial tumours. Journal of Feline Medicine and Surgery 27:1098612X251314336.

Doré M, 2011. Cyclooxygenase-2 expression in animal cancers. Veterinary Pathology 48:254–265.

Du X and Liu S, 2026. Targeted DNA methylation of the JSRV LTR suppresses Env-driven pulmonary adenocarcinoma: Epigenetic silencing as a potential veterinary therapeutic strategy. Veterinary Microbiology 313:110859.

Hodor D, Negoescu A, Pop R, *et al.*, 2026. Metastatic potential of ovine pulmonary adenocarcinoma: a comprehensive assessment of the draining pulmonary lymph nodes. Journal Of Veterinary Diagnostic Investigation: Official Publication of the American Association Of Veterinary Laboratory Diagnosticians, Inc. Advance online publication. p.10406387251409774.

Karakurt E, Beytut E, Dağ S, *et al.*, 2022a. Assessment of MDA and 8-OHdG expressions in ovine pulmonary adenocarcinomas by immunohistochemical and immunofluorescence methods. Acta Veterinaria Brno 91:235–241.

Karakurt E, Beytut E, Dağ S, *et al.*, 2022b. Immunohistochemical detection of pro-inflammatory and anti-inflammatory interleukins in the lungs of sheep with jaagsiekte. Turkish Journal of Veterinary Research 6:9-14.

Karakurt E, Beytut E, Dağ S, *et al.*, 2022c. Immunohistochemical detection of TNF-α and IFN-γ expressions in the lungs of sheep with pulmonary adenocarcinomas. Acta Veterinaria Eurasia 48:161-166.

Karakurt E, Beytut E, Dağ S, *et al.*, 2022d. The relationship between metastasis and MMP-9 in sheep with pulmonary adenocarcinomas. Kafkas Universitesi Veteriner Fakultesi Dergisi 28:211-216.

Karakurt E, Coşkun N, Beytut E, *et al.*, 2023. Evaluation of the relationship between inflammatory reaction and interleukins in ovine pulmonary adenocarcinomas. Veterinary Research Forum 14:1–6.

Karakurt E, Coşkun N, Keleş ÖF, *et al.*, 2025.Comparison of classical and atypical forms of ovine pulmonary adenocarcinomas using immunohistochemical and molecular techniques. Pakistan Veterinary Journal 45:1744-1754.

Lee AM, Wolfe A, Cassidy JP, *et al.*, 2017. First confirmation by PCR of Jaagsiekte sheep retrovirus in Ireland and prevalence of ovine pulmonary adenocarcinoma in adult sheep at slaughter. Irish Veterinary Journal 70:33.

Liu B, Qu L and Yan S, 2015. Cyclooxygenase-2 promotes tumor growth and suppresses tumor immunity. Cancer Cell International 15:106.

Liu X, Zhang J, Sun W, *et al.*, 2024. COX-2 in lung cancer: Mechanisms, development, and targeted therapies. Chronic Diseases and Translational Medicine 10:281–292.

Minguijón E, González L, De las Heras M, *et al.*, 2013. Pathological and aetiological studies in sheep exhibiting extrathoracic metastasis of ovine pulmonary adenocarcinoma (Jaagsiekte). Journal of Comparative Pathology 148:139-147.

Musser ML, Doke R, Viall AK, *et al.*, 2025. High expression of prostaglandin EP4 receptor mRNA in feline head and neck squamous cell carcinoma. Canadian Journal of Veterinary Research 89:113-119.

Ortega J, Corpa JM, Castillo D, *et al.*, 2023. Pathological spectrum of ovine pulmonary adenocarcinoma in small ruminants: A focus on the mixed form. Animals (Basel) 13:2828.

Palmarini M, Holland MJ, Cousens C, *et al.*, 1996. Jaagsiekte retrovirus establishes a disseminated infection of the lymphoid tissues of sheep affected by pulmonary adenomatosis. The Journal of General Virology 77:2991-2998.

Pu D, Yin L, Huang L, *et al.*, 2021. Cyclooxygenase-2 inhibitor: A potential combination strategy with immunotherapy in cancer. Frontiers in Oncology 11:637504.

Quintas H, Pires I, Garcês A, *et al.*, 2021. The diagnostic challenges of ovine pulmonary adenocarcinoma. Ruminants 1:58-71.

Reséndiz-Pozos RA, González-Saínz JM, Ortín A, *et al.*, 2025. Histopathological and immunohistochemical study of neoplastic cell heterogeneity in early and advanced ovine pulmonary adenocarcinoma. Animals (Basel) 15:2632.

Santelices Iglesias OA, Wright C, Duchene AG, *et al.*, 2018. Association between degree of anaplasia and degree of inflammation with the expression of COX-2 in feline injection site sarcomas. Journal of Comparative Pathology 165:45-51.

Scott PR, Dagleish MP and Cousens C, 2018. Development of superficial lung lesions monitored on farm by serial ultrasonographic examination in sheep with lesions confirmed as ovine pulmonary adenocarcinoma at necropsy. Irish Veterinary Journal 71:23.

Sun X, Du F and Liu S, 2017. Modulation of autophagy in exJSRV-env-transfected cells through the Akt/mTOR and MAPK signaling pathway. Biochemical and Biophysical Research Communications 485:672–678.

Toma C, Bâlteanu VA, Tripon S, *et al.*, 2020. Exogenous jaagsiekte sheep retrovirus type 2 (exJSRV2) related to ovine pulmonary adenocarcinoma (OPA) in Romania: prevalence, anatomical forms, pathological description, immunophenotyping and virus identification. BMC Veterinary Research 16:296.

Toma C, Popa R, Ciobanu L, *et al.*, 2025. Overexpression of IL-6 and STAT3 may provide new insights into ovine pulmonary adenocarcinoma development. BMC Veterinary Research 21:29.

Vieira TC, Oliveira EA, Santos BJD, *et al.*, 2022. COX-2 expression in mammary invasive micropapillary carcinoma is associated with prognostic factors and acts as a potential therapeutic target in comparative oncology. Frontiers in Veterinary Science 9:983110.

Wojtkowska A, Małek A, Giziński S, *et al.*, 2024. Comparison of MMP-2, MMP-9, COX-2, and PGP expression in feline injection-site and feline noninjection-site sarcomas-pilot study. Animals (Basel) 14:2110.

Xinyi L, Jinlong L and Bin Z, 2025. Low-invasive biomarkers of canine mammary tumours. Veterinary Medicine and Science 11:e70280.

Youssef G, Wallace WA, Dagleish MP, *et al.*, 2015. Ovine pulmonary adenocarcinoma: a large animal model for human lung cancer. ILAR Journal 56:99–115.

Zhang L, Yang H, Duan X, *et al.,* 2024. Modulation of autophagy affected tumorigenesis induced by the envelope glycoprotein of JSRV. Virology 594:110059.

Zhang P, Wang Y, Duan X, *et al.*, 2025. Exogenous Jaagsiekte sheep retrovirus (JSRV) Inner Mongolia strain: whole-genome characterization and viral particle packaging. Frontiers in Veterinary Science 12:1608822.